Saudi Pharmaceutical Journal 29 (2021) 981–991

Contents lists available at ScienceDirect

Saudi Pharmaceutical Journal

journal homepage: www.sciencedirect.com

Original article

Synthesis, *in vivo* and *in silico* analgesic and anti-inflammatory studies of α-D-ribofuranose derivatives

Sabiha Enam Spriha, Fahad Imtiaz Rahman, S. M. Abdur Rahman *

Department of Clinical Pharmacy & Pharmacology, Faculty of Pharmacy, University of Dhaka, Dhaka 1000, Bangladesh

ARTICLE INFO

Article history:
Received 7 February 2021
Accepted 16 July 2021
Available online 21 July 2021

Keyword:
α-D-ribofuranose
Analgesics
Anti-inflammatory agents
Chemical synthesis
Molecular docking simulation

ABSTRACT

Five α-D-ribofuranose analogues (**2**, **3**, **4, 5** and **6**) were synthesized in good yields from 3-*O*-benzyl-4-*C*-(hydroxymethyl)-1, 2-*O*-isopropylidene-α-D-ribofuranose (**1**). The synthesized compounds were then subjected to analgesic, anti-inflammatory, antimicrobial and antioxidant assays. Compound **3** demonstrated 79.74% ($P < 0.001$) writhing inhibition and highest reaction time of 2.55 ± 0.13 min ($P < 0.001$) after 30 min of oral administration in peripheral and central analgesic assay, respectively, at 50 mg/kg dose. Compound **2** and **6** exhibited significant anti-inflammatory activity at 100 mg/kg dose with paw edema inhibition of 91.15% ($P < 0.001$) and 95.13% ($P < 0.001$), respectively, in 4th hour. The synthesized analogues did not show notable antioxidant and antibacterial properties. Molecular docking study revealed higher binding affinity of −8.1 kcal/mol and −8.9 kcal/mol of compound **3** towards cyclooxygenase-1 and phospholipase A_2, respectively, compared to −7.7 and −7.6 kcal/mol respectively for corresponding native ligands. Compound **2** demonstrated binding affinity of −9.1 kcal/mol towards interleukin-1 receptor-associated kinase-4 compared to −8.7 kcal/mol of the native ligand. The molecular properties related to drug likeness of compounds were found to be within acceptable range. Synthesized D-ribofuranose analogues demonstrated promising analgesic and anti-inflammatory activities and further development may lead to new potent analgesic and anti-inflammatory agents.

1. Introduction

Ribose sugar is one of the most potent classes of carbohydrates due to versatile applications of its analogues (Adamo and Pergoli, 2008; Cappellacci et al., 2002; Shecterle et al., 2010). A great deal of D-ribose and D-ribofuranose analogues are used in the synthesis of nucleoside and nucleotide derivatives (Downey et al., 2015; Fujisaka et al., 2019; Komatsu and Araki, 2003; Rahman et al., 2009). Many of these nucleosides possess numerous biological activities and the sugar moiety within these compounds are required for exhibiting these effects (El-Gazzar et al., 2009). D-ribose itself (Fig. 1, structure **a**) has shown anti-inflammatory effect by reducing serum concentration of renal inflammatory biomarkers in mice (Ueki et al., 2013). It is also used in congestive heart failure as a supplementary therapy and has shown enhancement of diastolic performance in congestive heart failure cases (Omran et al., 2003; Wagner et al., 2009). Adding D-ribose in the treatment regimen of fibromyalgia syndrome caused improvement in clinical outcomes (Gebhart and Jorgenson, 2004; Teitelbaum, 2012). Ribofuranosides of some synthesized pyrimidine (Fig. 1, structure **b**) and phenothiazine analogues showed better antimicrobial activity than the analogues alone (Kumar et al., 2001). α-D-ribofuranose analogues and its nucleoside derivatives have many reported pharmacological properties including analgesic, anti-inflammatory, antimicrobial and cytotoxic effect (Galmarini et al., 2008; Petrelli et al., 2017; Rahman et al., 2020). Some triazole based D-ribofuranose (Ferreira et al., 2010) and recently isolated α-D-ribofuranose derivatives (for example structure **c** in Fig. 1) obtained from mangrove fungus (Zhang et al., 2021) exhibited α-glucosidase inhibitory activity.

Since D-ribose and its analogues showed several biological activities, we became interested to synthesize and investigate the biological properties of D-ribose derivatives. Recently, we have (Rahman et al., 2020) reported potential analgesic and anti-inflammatory activity of some known a-D-ribofuranose derivatives (structure **d,** Fig. 1). This result encouraged us to synthesize more derivatives and to evaluate their diverse biological properties via

* Corresponding author.
E-mail address: smarahman@du.ac.bd (S. M. Abdur Rahman).
Peer review under responsibility of King Saud University.

Production and hosting by Elsevier

https://doi.org/10.1016/j.jsps.2021.07.017
1319-0164/

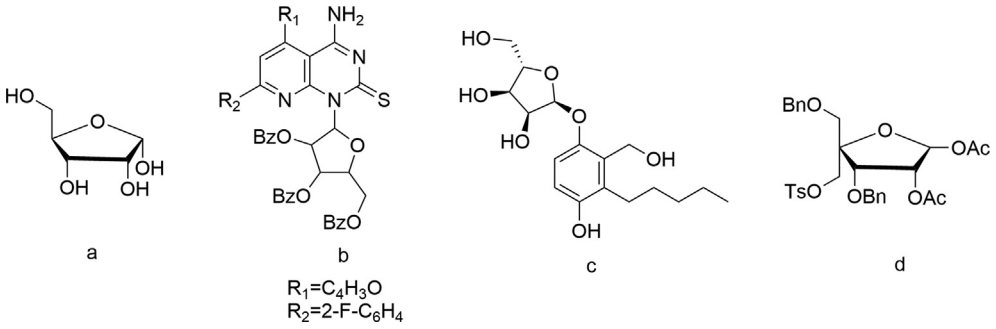

Fig. 1. Structure of α-D-ribose (a) and some bioactive α-D-ribofuranose derivatives (b-d).

in vitro and *in vivo* studies as well as *in silico* studies. Therefore, we attempted to synthesize some new derivatives of α-D-ribofuranose in order to investigate their pharmacological properties. In addition, we also examined the biological activity of the previously reported derivatives which had not been accomplished before. Thus, this study is directed to synthesize some known and unknown derivatives of α-D-ribofuranose, to characterize the synthesized molecules by spectroscopic methods and to evaluate their hitherto unknown pharmacological and biological properties. The study also involves an attempt to find the binding affinity of the synthesized compounds against target macromolecules by molecular docking and to see if results are consistent with *in vivo* results. The molecular properties that affect the drug likeness of compounds, for instance, molecular weight, hydrogen bond acceptors and donors, lipophilicity, molar refractivity were also assessed by *in silico* approach.

2. Materials and methods

2.1. Chemicals and equipment

The starting compound of this study is a derivative of α-D-ribofuranose known as 3-*O*-benzyl-4-*C*-(hydroxymethyl)-1, 2-*O*-isopropylidene-α-D-ribofuranose which is widely utilized for synthesizing bridged nucleoside analogues (Hari et al., 2002; Rahman et al., 2008; Sharma et al., 2015). Chemicals and solvents applied in the synthetic procedures were procured from either Sigma-Aldrich (USA) or Merck (Germany). Solvents were further purified by drying over CaH_2 and distillation. All glassware was well dried before each reaction. The completion of chemical reactions was detected by thin layer chromatography (TLC) in befitting solvent system. Column chromatography with silica gel 60–120 mesh (Lobachemie, India) was employed to purify crude products. Fourier-transform infrared (FTIR) spectra were recorded from Centre of Advanced Research in Science, University of Dhaka with FTIR spectrophotometer (IRPrestige 21, Shimadzu Corporation, Japan). Proton and carbon nuclear magnetic resonance i.e. ^{1}H NMR and ^{13}C NMR spectra were produced on Bruker (Burker AMX-400) or JNM-ECS-300 (JEOL) spectrometers. Mass spectra were recorded using matrix assisted laser desorption/ionization coupled to time of flight (MALDI-TOF) technique in Spiral TOF JMS-S3000 instrument (JEOL).

*2.2. Synthesis of 3, 5-di-O-benzyl-4-C-(hydroxymethyl)-1, 2-O-isopropylidene-α-D-ribofuranose (**2**)*

Sodium hydride (0.93 g, 38.60 mmol) was taken into the solution of the starting material **1** (6 g, 19.30 mmol) in dimethyl formamide (80 ml) and benzyl bromide (2.50 ml, 21.20 mmol) at 0 °C. The reaction mixture was then stirred under a N_2 atmosphere to prevent moisture interference for 8 h at room temperature. After the completion of the reaction, the reaction mixture was quenched by adding ice cold water (100 ml) and the resulting mixture was extracted by ethyl acetate (3x100 ml). The extract was washed with water, dried over sodium sulfate and concentrated. Column chromatography (n-hexane: ethyl acetate = 3:1) of the concentrated residue yielded the product **2** as a transparent oil. Yield: 4.2 g, 53.26%; R_f = 0.30 (*n*-hexane: ethyl acetate = 2:1); IR (thin film, cm^{-1}): 3570 (O—H), 2940–2870 (C—H), 1452 (C═C, aromatic), 739 (C—H, aromatic); ^{1}H NMR (400 MHz, $CDCl_3$, δ/ppm): 1.35 (s, 3H), 1.636 (s, 3H), 3.54 (d, *J* = 10.4 Hz, 1H), 3.61 (d, *J* = 10.4 Hz, 1H), 3.83 (d, *J* = 12 Hz, 1H), 3.94 (d, *J* = 12 Hz, 1H), 4.28 (d, *J* = 5.2 Hz, 1H), 4.56 (m, 4H), 4.65 (s, 1H), 4.78 (d, *J* = 11.6 Hz, 1H), 5.79 (d, *J* = 3.6 Hz, 1H), 7.34 (m, 10*H*).

*2.3. Synthesis of 4-C-(acetoxymethyl)-3, 5-di-O-benzyl-1, 2-O-isopropylidene-α-D-ribofuranose (**3**)*

Pyridine (1.20 ml, 15 mmol) was added in a dried vessel containing compound **2** (3 g, 7.5 mmol) in acetic anhydride (2.10 ml, 22.50 mmol) under fume-hood and was stirred for 3 h at room temperature. After diluting the reaction with water, the organic phase was extracted by ethyl acetate (3x100 ml) and concentrated using a rotatory evaporator. The concentrate was then co-evaporated with 20 ml toluene to remove excess pyridine. Column chromatography (*n*-hexane: ethyl acetate = 3:1) of the residue produced purified product **3** as a transparent oil. Yield: 2.78 g, 83.7%; R_f = 0.57 (n-hexane: ethyl acetate = 2:1); IR (thin film, cm^{-1}): 3028 (C—H, aromatic), 2870 (C—H), 1738 (C═O, ester), 1449 (C═C, aromatic), 741 (C—H, Aromatic); ^{1}H NMR (400 MHz, $CDCl_3$, δ/ppm): 1.33 (s, 3H), 1.62 (s, 3H), 2.03 (s, 3H), 3.45 (d, *J* = 10.4 Hz, 1H), 3.56 (d, *J* = 10.8 Hz , 1H), 4.26 (d, *J* = 5.2 Hz, 1H), 4.31 (d, *J* = 12 Hz, 1H), 4.44 (d, *J* = 12 Hz, 1H), 4.54 (d, *J* = 10.4 Hz, 2H), 4.64 (d, *J* = 12.4, 2H), 4.74 (d, *J* = 12 Hz, 1H), 5.77 (d, *J* = 3.6 Hz 1H), 7.30 (m, 9H), 7.24 (d, *J* = 8 Hz, 1H).

*2.4. Synthesis of 3, 5-di-O-benzyl-4-C-(hydroxymethyl)-O-methyl - D-ribofuranose (**4**)*

Water (6.00 ml) and methanol (12.00 ml) and 28% HCl (31.00 ml) were added sequentially in a vessel containing **3** (1.5 g, 3.39 mmol) and was stirred at room temperature for 19 h. The organic phase extraction was carried out with ethyl acetate (3 × 100 ml), washed with brine and dried over anhydrous sodium sulfate. The concentrated residue was subjected to column chromatography (*n*-hexane: ethyl acetate = 3:1) to acquire the purified product **4** as a transparent oil. Yield: 1.01 g, 79.56%); R_f = 0.18 (*n*-hexane: ethyl acetate = 2:1); IR (thin film, cm^{-1}): 3390–3317 (O—H), 3031 (C-H, aromatic), 2930–2863 (C—H), 1454 (C═C, aromatic), 1044 (C—O), 1101 (C—O), 738 (C—H, aromatic); ^{1}H NMR (300 MHz, $CDCl_3$, δ/ppm): 3.28 (s, 3H), 3.39 (d, *J* = 9.6 Hz, 1H),

3.41 (d, *J* = 7.2 Hz, 1H), 3.43 (d, *J* = 9.6 Hz, 1H), 3.76 (d, *J* = 12.0 Hz, 1H), 3.90 (d, *J* = 12.0 Hz , 1H), 4.06–4.13 (m, 2H), 4.50 (d, *J* = 11.7 Hz, 1H), 4.52–4.57 (m, 3H), 4.72 (d, *J* = 11.7 Hz, 1H), 4.87 (s, 1H), 7.27–7.37 (m, 10*H*). ^{13}C NMR (75 MHz, $CDCl_3$, δ/ppm): 54.94, 62.97, 72.58, 72.95, 73.72, 74.69, 81.23, 85.87, 108.35, 127.75 (2C), 127.89 (2C), 128.08 (2C), 128.54 (2C), 128.59 (2C), 137.56, 137.98. HRMS (MALDI-TOF) *m*/*z*: $[M+Na]^+$ calculated for $C_{21}H_{26}O_6$-Na 397.1627; found 397.1622.

2.5. Synthesis of 4-C-(acetoxymethyl)-3, 5-di-O-benzyl-O-methyl - D-ribofuranose (**5**)

Pyridine (0.40 ml, 5 mmol) was added in a dried vessel containing compound **4** (0.90 g, 2.40 mmol). Acetic anhydride (0.23 ml, 2.40 mmol) was added to the mixture under fume-hood and was stirred for 3 h at room temperature. After quenching the reaction with water, the organic phase was extracted by ethyl acetate (3 × 100 ml), washed with brine and concentrated using a rotatory evaporator. The concentrate was then co-evaporated with 20 ml toluene to eliminate excess pyridine. Column chromatography (*n*-hexane: ethyl acetate = 3:1) of the residue produced purified product **5** as a transparent oil. Yield: 0.85 g, 85.04%; R_f = 0.25 (n-hexane: ethyl acetate = 2:1); IR (thin film, cm^{-1}): 3318 (O—H), 3032 (C—H, aromatic), 2932–2864 (C-H), 1741 (C═O, ester), 1454 (C═C, aromatic), 739 (C-H, aromatic); ^{1}H NMR (400 MHz, $CDCl_3$, δ/ppm): 2.10 (s, 3H), 3.33 (s, 3H), 3.37–3.41 (m, 2H), 3.39 (d, *J* = 9.2 Hz, 1H), 3.46 (br s, 1H), 3.64 (d, *J* = 9.2 Hz, 1H), 4.10 (d, *J* = 5.0 Hz, 1H), 4.23 (d, *J* = 5 Hz , 1H), 4.31 (d, *J* = 11.9 Hz, 1H), 4.50 (d, *J* = 11.9 Hz, 1H), 4.58 (d, *J* = 3.2 Hz, 1H), 4.67 (d, *J* = 4.2 Hz, 1H), 4.91 (s, 1H), 7.31–7.41 (m, 10*H*). ^{13}C NMR (100 MHz, $CDCl_3$, δ/ppm): 20.99, 54.98, 64.67, 72.92, 73.43, 73.59, 73.85, 81.35, 83.75, 107.85, 127.68 (2C), 127.73(2C), 127.78, 128.03, 128.43 (2C), 128.51(2C), 137.29, 137.85, 170.37. HRMS (MALDI-TOF) *m*/*z*: $[M+Na]^+$ calculated for $C_{23}H_{28}O_7Na$ 439.1733; found 439.1725.

2.6. Synthesis of 3-O-benzyl-4-C-(hydroxymethyl)-D-ribofuranose (**6**)

Compound **1** (0.50 g, 1.61 mmol) in 50% (w/v) acetic acid (1.94 ml, 16.1 mmol) was kept stirring at room temperature for 2 h. The organic phase was extracted using ethyl acetate (3 × 100 ml), washed with water and dried over anhydrous sodium sulfate. The organic phase was then concentrated using a rotatory evaporator. Finally, the product **5** was purified as a transparent oil by column chromatography (*n*-hexane: ethyl acetate = 1:99). Yield: 0.293 g, 67.7%; R_f = 0.16 (*n*-hexane: ethyl acetate = 1:99); IR (thin film, cm^{-1}) 3391–3318 (O—H), 2930–2878 (C—H), 1456 (C═C, aromatic ring), 745 (C—H, aromatic); ^{1}H NMR (400 MHz, DMSO d_6, δ/ppm): 3.09 (m, 2H), 3.45 (m, 2H), 3.62 (m, 1H), 3.84 (d, *J* = 11.6 Hz, 1H), 4.42 (m, 2H) , 4.65 (m, 2H), 4.85 (m, 2H), 6.29 (m, 1H), 7.21 (m, 5H). ^{13}C NMR (75 MHz, $CDCl_3$, δ/ppm): 62.67, 65.01, 68.40, 71.10, 73.21, 80.05, 95.09, 127.28, 127.53 (2C), 128.16 (2C), 139.09. HRMS (MALDI-TOF) *m*/*z*: $[M+Na]^+$ calculated for $C_{13}H_{18}O_6Na$ 293.1001; found 293.0991.

2.7. Animals

Swiss albino mice (*Mus musculus)* of around 25–30 g of either sex having age range of around 4–5 weeks, collected from Jahangirnagar University were used for investigation. Animals were used in experiments in lowest possible numbers maintaining the ethical standards and guidelines devised by Swiss Academy of Medical Sciences. Ethics committee approval number: Ref: DU/Pharm_ETA: 01_09/2019.

2.8. Analgesic activity

2.8.1. Acetic acid induced writhing method

Acetic acid induced writhing method was utilized with minute changes to investigate peripheral analgesic effect (Faujdar et al., 2016). Sixty mice were designated into twelve separate equal groups randomly. Negative control group was given 0.9% NaCl, positive control group received diclofenac (25 mg/kg) while all other groups received synthesized compounds (25 and 50 mg/kg) orally. After forty minutes, acetic acid (0.7% v/v, 10 ml/kg) was administered in intraperitoneal route to all groups to prompt writhing. Writhing count started five minutes later and was noted for the next fifteen minutes for every mouse.

2.8.2. Tail immersion method

The central anti-nociception activities of the synthesized compounds were investigated by tail immersion method using a hot water bath of 55 °C (Faujdar et al., 2016). Sixty mice were separated into twelve equal groups. In this test, positive control group was treated with morphine (2 mg/kg), negative control group with 0.9% NaCl and other groups with synthesized compounds (25 and 50 mg/kg). The tail flicking time was measured at different time intervals (0, 30, 60 and 90 min). Doses for both the tests were chosen after conducting a pilot study where mice were given different levels of test materials ranging from 5 to 400 mg/kg. Doses with significant analgesic activity and low noxious effects were selected.

2.9. Anti-inflammatory activity

Carrageenan induced hind paw edema method with few modifications was applied to assess anti-inflammatory activities of the compounds (Chung et al., 2016). Thirty-five Wister rats were designated into seven equal groups randomly. Negative control group was fed 0.9% NaCl while positive control group received aceclofenac (100 mg/kg). Test groups were given different synthesized derivative (100 mg/kg) as fine suspension orally. The volume of right hind paw was estimated using a plethysmometer at 0th hour (before carrageenan injection). This acted as baseline reading. After 1 h of oral administration, 1% carrageenan solution (0.1 ml) was administered into the right hind paw of mice of all groups. At 1, 2, 3 and 4 h after the carrageenan administration, paw volumes were estimated. Mean increase in the volume of hind paw and percentage inhibition of the volume was calculated for the respective time intervals. Dose of the synthesized compounds were chosen based on the usual dosage of aceclofenac and a similar pilot study as in analgesic activity test described in Section *2.8.2*.

2.10. Antimicrobial activity

Disk diffusion method was used to determine the antibacterial as well as antifungal capability of the synthesized compounds (Adukwu et al., 2016). Pre-sterilized disks of 6 mm diameter were diffused with 400 μg/disk of synthesized compounds and were transferred to petri-dishes cultured with different bacterial and fungal species. The bacterial species contained both Gram (+) species such as *Bacillus subtilis, Bacillus megaterium, Bacillus cereus, Sarcina lutea, Staphylococcus aureus* and Gram (−) species such as *Shigella dysenteriae, Shigella boydi, Pseudomonas aeruginosa, Escherichia coli, Salmonella typhi*, *Salmonella paratyphi, Vibrio parahemolyticus and Vibrio mimicus*. The fungal species used were *Candida albicans, Aspergilla niger* and *Saccharomyces cerevisiae.* Blank disks were used as negative control to ensure that the residual solvents and the filter paper with which the disks were made are not active themselves. The zones of inhibition were observed and compared to the standard ciprofloxacin disk and griseofulvin disk (10 μg/disk).

2.11. Antioxidant activity

The antioxidant property of the test samples was evaluated by percent inhibition of DPPH (2, 2-diphenyl-1-picrylhydrazyl) free radical where ascorbic acid was used as standard (Ahmed et al., 2019). Concentration of the compound that provides 50% inhibition or reduction of DPPH, also known as IC_{50} was calculated from the equation of the percentage inhibition versus concentration of the sample logarithmic curve.

2.12. Statistical analysis

Calculations were performed using XLSTAT software for Microsoft Excel 2013. Values were shown as the mean ± standard error of mean (SEM). One-way analysis of variance (ANOVA) and Dunnett's test were carried out where $P < 0.05$ was regarded as statistically significant.

2.13. Molecular docking simulation

The structure of proteins phospholipase A_2 ($PLA_{2)}$ (PDB code: 4UY1), cyclooxygenase-1 (COX-1) (PDB code: 1EQG), cyclooxygenase-2 (COX-2) (PDB code: 5IKT), NF-κB–inducing kinase (NIK) (PDB code: 4IDV) , interleukin-1 receptor associated kinase-4 (IRAK-4) (PDB code: 5KX7) was collected from Research Collaboratory for Structural Bioinformatics Protein Data Bank (RCSB PDB) (Berman et al., 2002). Energy minimization of ligands was performed in Open Babel (version 2.4.0) (O'Boyle et al., 2011). Validation of docking procedure was done by re-docking the native ligands in the binding pockets of respective proteins. The target protein–ligand docking was executed using AutoDock Vina (version 1.1.2) (Trott and Olson, 2009). Docking simulation was done using grid with its centers positioned at the active site of respective proteins and the dimensions of the grid were 25.00, 25.00, 25.00 Å. The interactions of ligands with target macromolecules were analyzed by Discovery Studio Client 2019.

2.14. Lipinski's rule of five prediction

Molecular weight, hydrogen bond donors and acceptors, lipophilicity, molar refractivity of the synthesized compounds were calculated using SwissADME (Daina et al., 2017).

3. Results

3.1. Synthesis of α-D-ribofuranose derivatives

Ribofuranose derivatives were synthesized from the starting material 3-*O*-benzyl-4-*C*-(hydroxymethyl)-1, 2-*O*-isopropylidene-α-D-ribofuranose (**1**) (Scheme 1). Compound **1** was subjected to benzylation at room temperature which yielded di-benzyl derivative **2** along with an undesired tri-benzyl derivative similar to that reported in our previous study (Rahman et al., 2020). Compound **2** was separated from the undesired product and reacted with acetic anhydride to produce acetylated derivative **3** in high yield. Acidic hydrolysis of compound **3** with 28% HCl followed by methylation produced compound **4** in good yield with additional removal of acetyl group. Compound **4** was acetylated using reaction conditions similar to previous acetylation. Compound **6** was also synthesized by hydrolytic cleavage of isopropylidene ring of the starting material **1**. The structures of the synthesized compounds were established by FTIR, ^{1}H NMR, ^{13}C NMR and mass spectra as presented in Sections *2.2*, *2.3*, *2.4*, *2.5* and *2.6*. Compound **2** and **3** were known compounds which were confirmed by comparing the spectral data with the reported data (Koshkin et al., 1998).

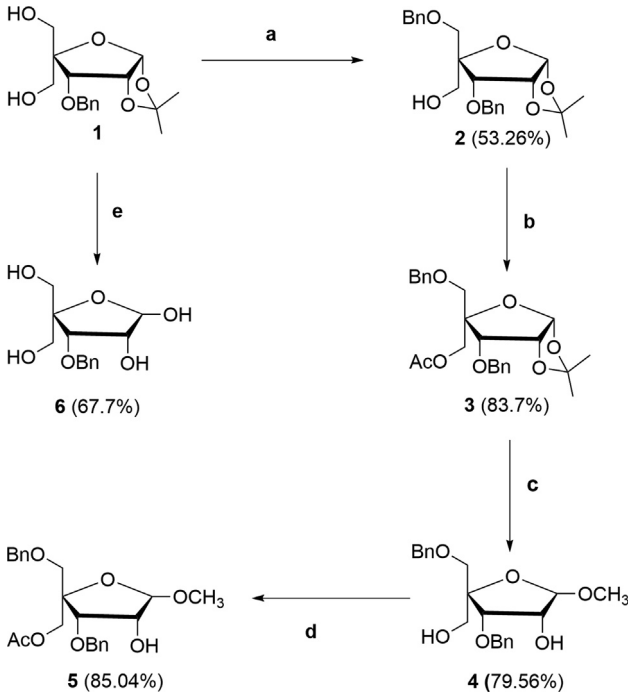

Scheme 1. Synthesis scheme for α-D-ribofuranose analogues. Reagents and conditions: (a) NaH, BnBr, DMF, 0 °C to rt, 8 h, (b) Ac_2O, pyridine, rt, 3 h, (c) 28% HCl, MeOH, H_2O, rt, 19 h, (b) Ac_2O, pyridine, rt, 3 h, (d) 50% AcOH, rt, 2 h.

3.2. Analgesic activity of synthesized compounds

3.2.1. Acetic acid induced writhing method

The peripheral analgesic property of synthesized compounds was investigated by acetic acid induced writhing method. The effects of the synthesized compounds to subside the pain caused by acetic acid are presented in Table 1. In this method compound **3** showed potent analgesic activity with inhibition of writhing of 54.74% and 79.74% at doses of 25 mg/kg and 50 mg/kg, respectively, whereas diclofenac as positive control at dose of 25 mg/kg inhibited writhing by 83.19%. At 50 mg/kg dose compound **2**, **4** and **5** showed writhing inhibition of 63.36%, 59.91% and 53.45%, respectively. Compound **6** at both doses showed mild analgesic activity compared to other test compounds.

3.2.2. Tail immersion method

The changes in sensitivity of test animals due to the analgesic activity of the test compounds were compared by tail flick method

Table 1
Analgesic activity of synthesized compounds in acetic acid induced writhing method.

Treatment (mg/kg)	Average writhing	Inhibition of writhing (%)
Control (–)	23.20 ± 0.30	–
Diclofenac (25)	3.90 ± 0.19***	83.19
2 (25)	13.40 ± 0.37***	42.24
2 (50)	8.50 ± 0.22***	63.36
3 (25)	10.50 ± 0.27***	54.74
3 (50)	4.70 ± 0.26***	79.74
4 (25)	14.60 ± 0.40***	37.07
4 (50)	9.30 ± 0.25***	59.91
5 (25)	17.20 ± 0.52***	25.86
5 (50)	10.80 ± 0.26***	53.45
6 (25)	20.50 ± 0.71**	11.64
6 (50)	17.60 ± 0.86***	24.14

Writhing counts are expressed as mean ± SEM, (n = 5). ***P < 0.001, **P < 0.01, *P < 0.05 compared with negative control (one-way ANOVA followed by Dunnett's test).

and the data are presented in Fig. 2**.** Compound **3** at the dose 50 mg/kg showed highest tail flicking reaction time of 2.55 ± 0.1 3 min after 30 min of oral administration among the test compounds which is comparable to morphine's 3.28 ± 0.15 min. Compound **3** at 25 mg/kg and compound **2** at 50 mg/kg dose showed reaction time of 2.00 ± 0.16 and 1.74 ± 0.12 min, respectively, after 30 min of oral administration. After 60 min of oral administration, compound **3** at 25 mg/kg and 50 mg/kg showed reaction time of 1.51 ± 0.11 and 2.03 ± 0.16 min which is superior to other test compounds at the same dose and same time interval.

3.3. Anti-inflammatory activity of synthesized compounds

The mean paw volume (ml) and percentage of paw edema inhibition of the compounds are shown in Table 2**.** From the statistical evaluation, it is evident that all the compounds at 100 mg/kg dose showed reduction of paw volume from the first hour and onwards. All the compounds showed anti-inflammatory activity among which compound **2** and **6** had prominent activity. The paw edema inhibition of compound **2** was 15.79%, 58.68%, 77.32% and 91.15% and compound **6** was 14.29%, 58.68%, 79.38% and 95.13% in 1st, 2nd, 3rd and 4th hour, respectively, whereas paw edema inhibition was 31.58%, 70.66%, 86.08% and 97.79% in 1st, 2nd, 3rd and 4th hour, respectively, for positive control aceclofenac (100 mg/kg). Compound **3, 4** and **5** also showed significant reduction in paw edema volume.

3.4. Antimicrobial and antioxidant activity of synthesized compounds

Antimicrobial activity of the compounds **2**, **3**, **4, 5** and **6** were assessed by disk diffusion method on both Gram-positive and Gram-negative species. DPPH free radical scavenging method was applied to determine the antioxidant potential of the compounds. However, the synthesized compounds did not show notable antimicrobial and antioxidant properties (data not shown).

3.5. Molecular docking simulation

Molecular docking studies showed that the binding affinities of compound **2, 3**, **4** and **5** with PLA_2 were greater than the native ligand's binding affinity, meaning PLA_2 may be a target for these compounds for their anti-inflammatory activity. Compound **3** effectively interacted with PLA_2 by forming hydrogen bond with Gly28A and Lys61A residue shown in Fig. 3**.** Among the four compounds, compound **3** had the highest affinity towards COX-1 which is also higher than the native ligand ibuprofen's binding affinity. Compound **3** formed hydrogen bond with Arg120A residue of COX-1 as depicted in Fig. 4 and this Arg120A residue is required for high affinity binding of arachidonic acid with cyclooxygenase (Vecchio et al., 2012). These interactions of compound **3** with PLA_2 and COX-1 may be accounted for significant anti-inflammatory and analgesic activity of this compound in biological study. However, the compounds showed lesser affinity towards COX-2 than COX-1 and binding patterns of the compounds with COX-2 are shown in Fig. 5**.** Compound **2** and **5** effectively bound with NIK as illustrated in Fig. 6 with binding affinities which are comparable to that of corresponding native ligand. Compound **2** formed hydrogen bond with Ser328B residue of IRAK-4 ATP binding site shown in Fig. 7 and had higher binding affinity than that of corresponding native ligand and other synthesized compounds. The binding affinities of synthesized molecules with these target proteins are shown in Table 3.

3.6. Lipinski's rule of five prediction

Molecular weight, octanol–water partition coefficient, number of hydrogen bond donor, number of hydrogen bond acceptor and molar refractivity properties for the synthesized compounds are presented in Table 4. All the compounds **2**, **3**, **4, 5** and **6** passed the Lipinski's rule of five screening with no violation of any of the acceptance criteria.

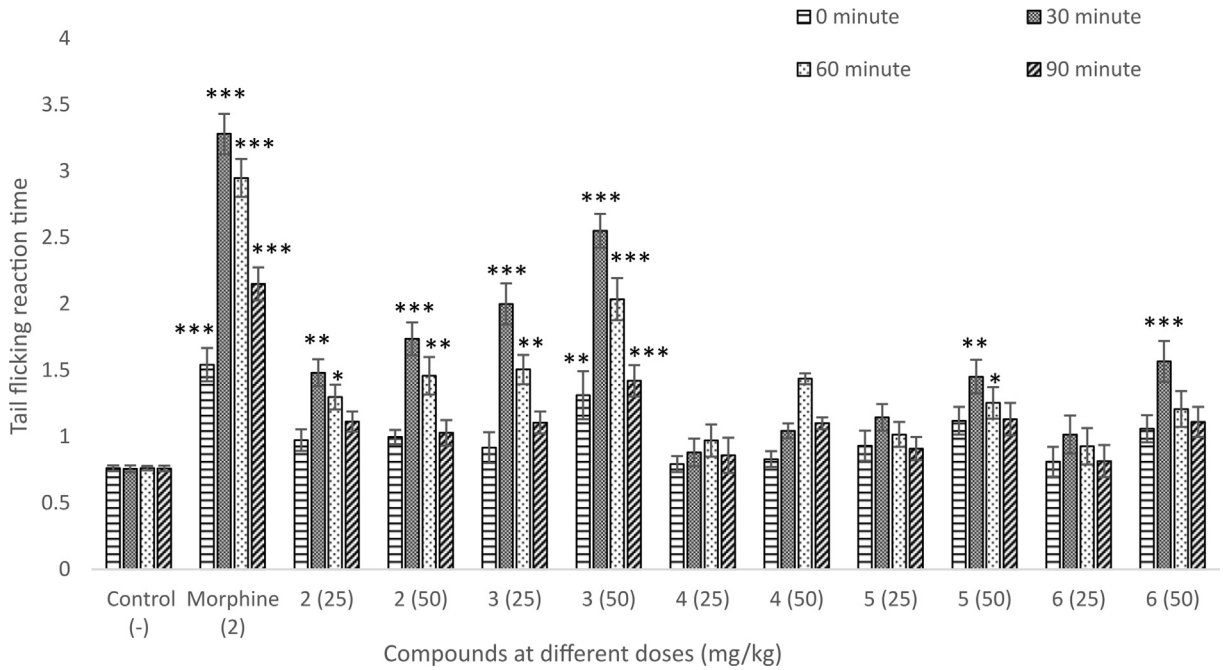

Fig. 2. Evaluation of central analgesic effect of synthesized compounds at doses 25 mg/kg and 50 mg/kg using tail flick method in mice where morphine was used as a standard. Reaction time values are expressed as mean ± SEM, (n = 5). $^{***}P < 0.001$, $^{**}P < 0.01$, $^{*}P < 0.05$ indicate significant differences when compared with negative control (one way ANOVA followed by Dunnett's test).

Table 2
Anti-inflammatory effect of different groups in carrageenan induced paw edema test.

Treatment (mg/kg)	Mean Paw Volume (ml) (inhibition of edema %)				
	Basal	1st hr	2nd hr	3rd hr	4th hr
Control (–)	0.57 ± 0.02	0.83 ± 0.01	0.90 ± 0.02	0.96 ± 0.02	1.02 ± 0.03
Aceclofenac (100)	0.51 ± 0.01	0.69 ± 0.01*** (31.58)	0.61 ± 0.02*** (70.66)	0.56 ± 0.03*** (86.08)	0.52 ± 0.02*** (97.79)
2 (100)	0.51 ± 0.02	0.73 ± 0.02** (15.79)	0.64 ± 0.02*** (58.68)	0.60 ± 0.02*** (77.32)	0.55 ± 0.02*** (91.15)
3 (100)	0.52 ± 0.01	0.76 ± 0.02 (11.28)	0.70 ± 0.02*** (46.71)	0.65 ± 0.02*** (67.01)	0.58 ± 0.02*** (86.73)
4 (100)	0.57 ± 0.02	0.80 ± 0.03 (13.53)	0.71 ± 0.03*** (58.08)	0.67 ± 0.03*** (73.71)	0.63 ± 0.04*** (88.00)
5 (100)	0.56 ± 0.01	0.80 ± 0.02 (12.03)	0.74 ± 0.01*** (46.71)	0.70 ± 0.02*** (63.40)	0.66 ± 0.02*** (78.32)
6 (100)	0.52 ± 0.01	0.74 ± 0.02** (14.29)	0.65 ± 0.02*** (58.68)	0.60 ± 0.02*** (79.38)	0.54 ± 0.01*** (95.13)

Paw volume values are presented as mean ± S.E.M. (n = 5); ***P < 0.001, **P < 0.01, *P < 0.05 compared to control (–) by Dunnett's test.

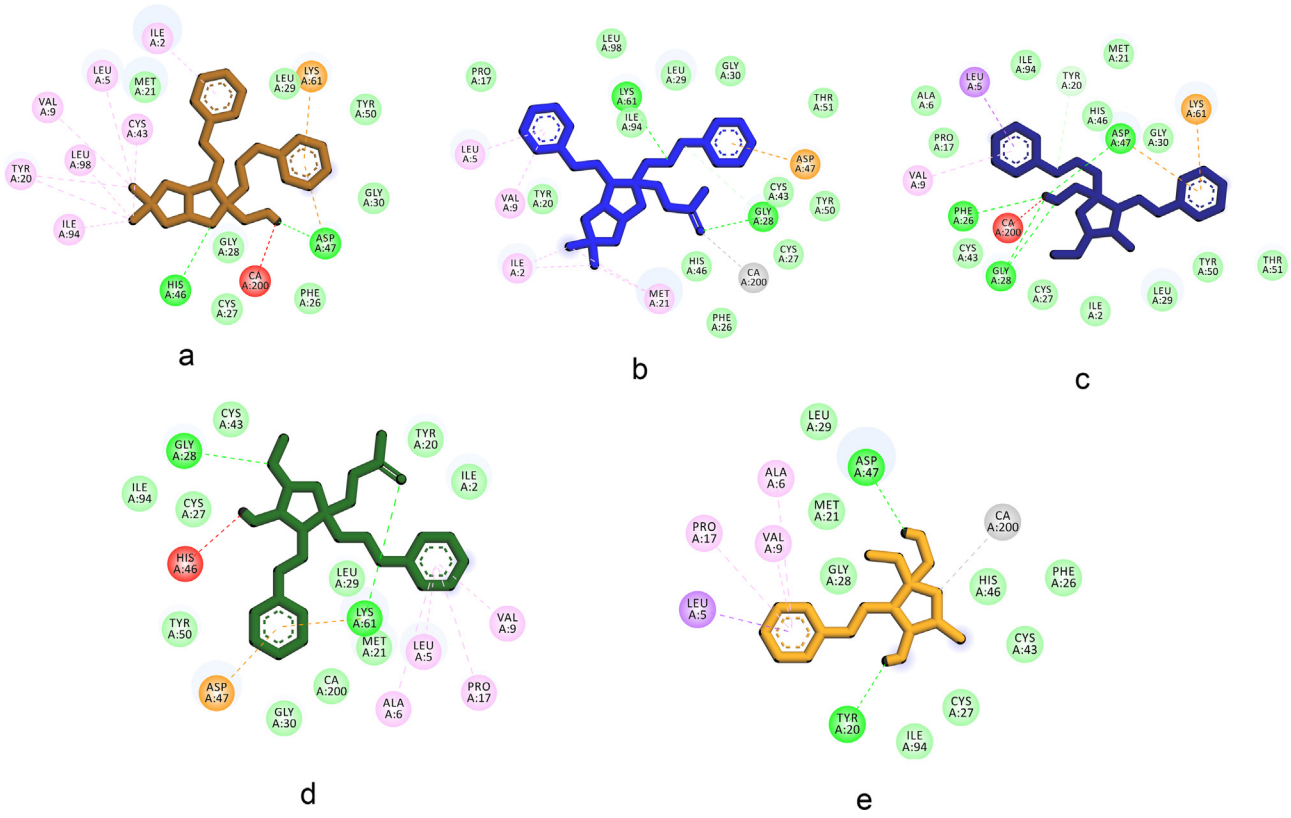

Fig. 3. Interaction of synthesized compounds (a) **2**, (b) **3**, (c) **4**, (d) **5** and (e) **6** with PLA_2 (4UY1) active site. Green: conventional hydrogen bond; pink-violet: hydrophobic; light green: Van der Waals; cyan: carbon hydrogen; orange: pi-anion/pi-cation; grey: metal acceptor; red: electron donor–donor interaction.

4. Discussion

In the current study synthesized α-D-ribofuranose derivatives were subjected to various pharmacological screening. Analgesic activity of synthesized compounds was evaluated by two different methods. In acetic acid induced writhing method, intra peritoneal administration of acetic acid prompts an acute inflammatory response followed by activation of the nociceptors (Dzoyem et al., 2017). The tail flick method is also broadly applied to assess anti-nociceptive property of compounds. Exposing the tail of mice to heat activates heat sensitive receptors, transient receptor potential vanilloid type 1 and 3 (TRPV1 and TRPV3) receptors promoting pain transmission (Leksiri et al., 2020). Compound **3** exhibited potent analgesic activity in both the tests. Compound **2**, **4** and **5** also exhibited moderate analgesic activity in both the tests. Analgesic activity of compound **3**, **4** and **5** is reported for the first time in this study. D-ribose derivatives and several nucleoside analogues containing modified ribose has exhibited notable anti-nociceptive effect (El-Gazzar et al., 2009; Gebhart and Jorgenson, 2004; Jarvis et al., 2002; Ueki et al., 2013). Structural resemblance

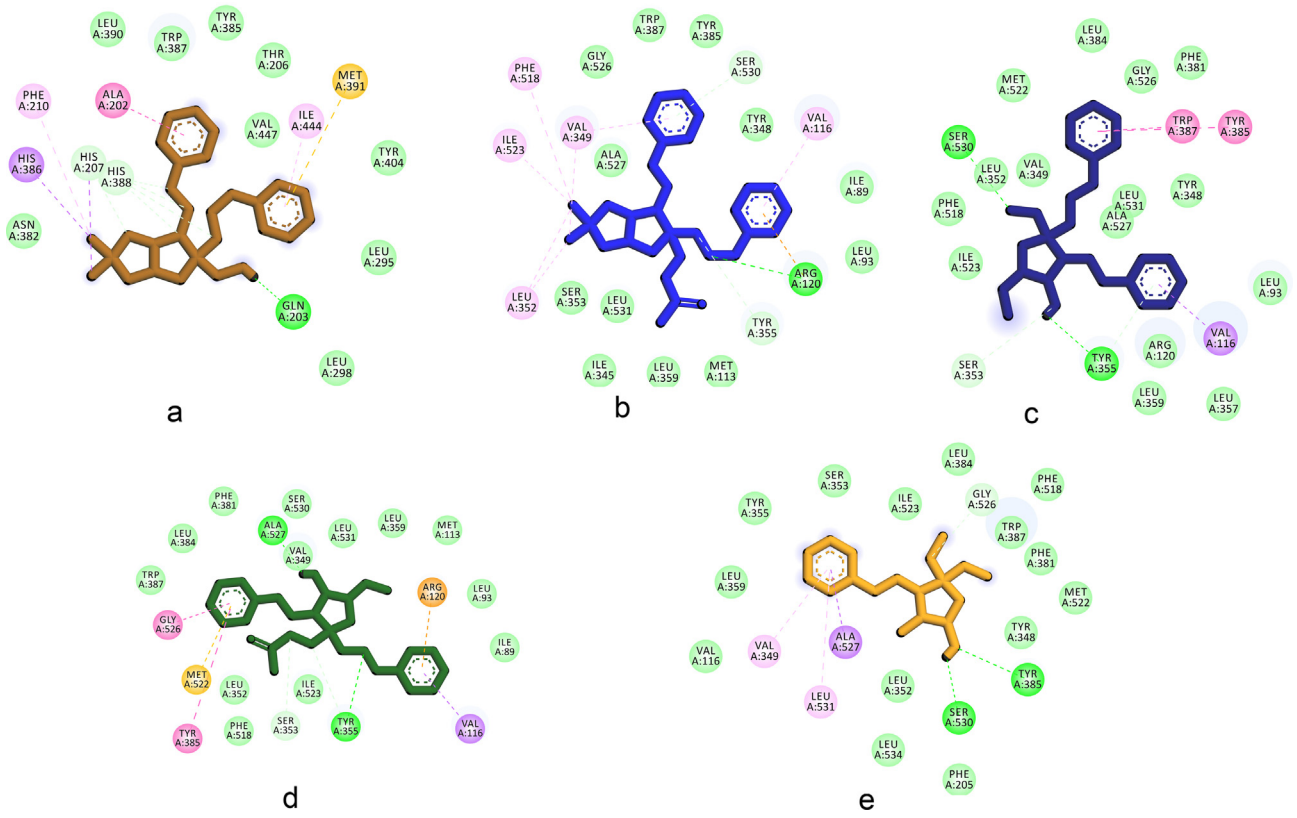

Fig. 4. Interaction of synthesized compounds (a) **2**, (b) **3**, (c) **4**, (d) **5** and (e) **6** with COX-1 (1EQG) active site. Green: conventional hydrogen bond; pink-violet: hydrophobic; light green: Van der Waals; cyan: carbon hydrogen bond/ pi-donor hydrogen bond; orange: pi-cation; brown: pi-sulfur interaction.

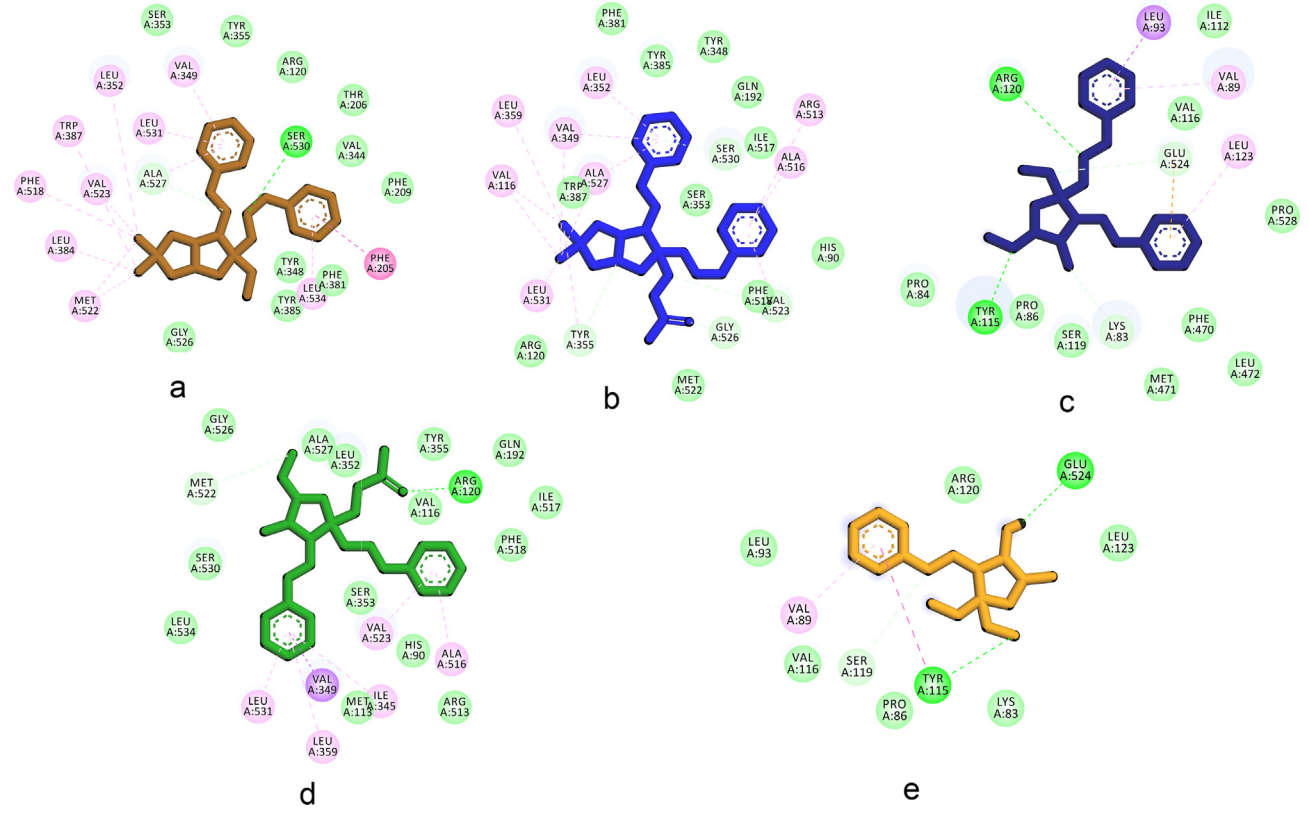

Fig. 5. Interaction of synthesized compounds (a) **2**, (b) **3**, (c) **4**, (d) **5** and (e) **6** with COX-2 (5IKT) active site. Green: conventional hydrogen bond; pink-violet: hydrophobic; light green: Van der Waals; cyan: carbon hydrogen bond/ pi-donor hydrogen bond; orange: pi-anion interaction.

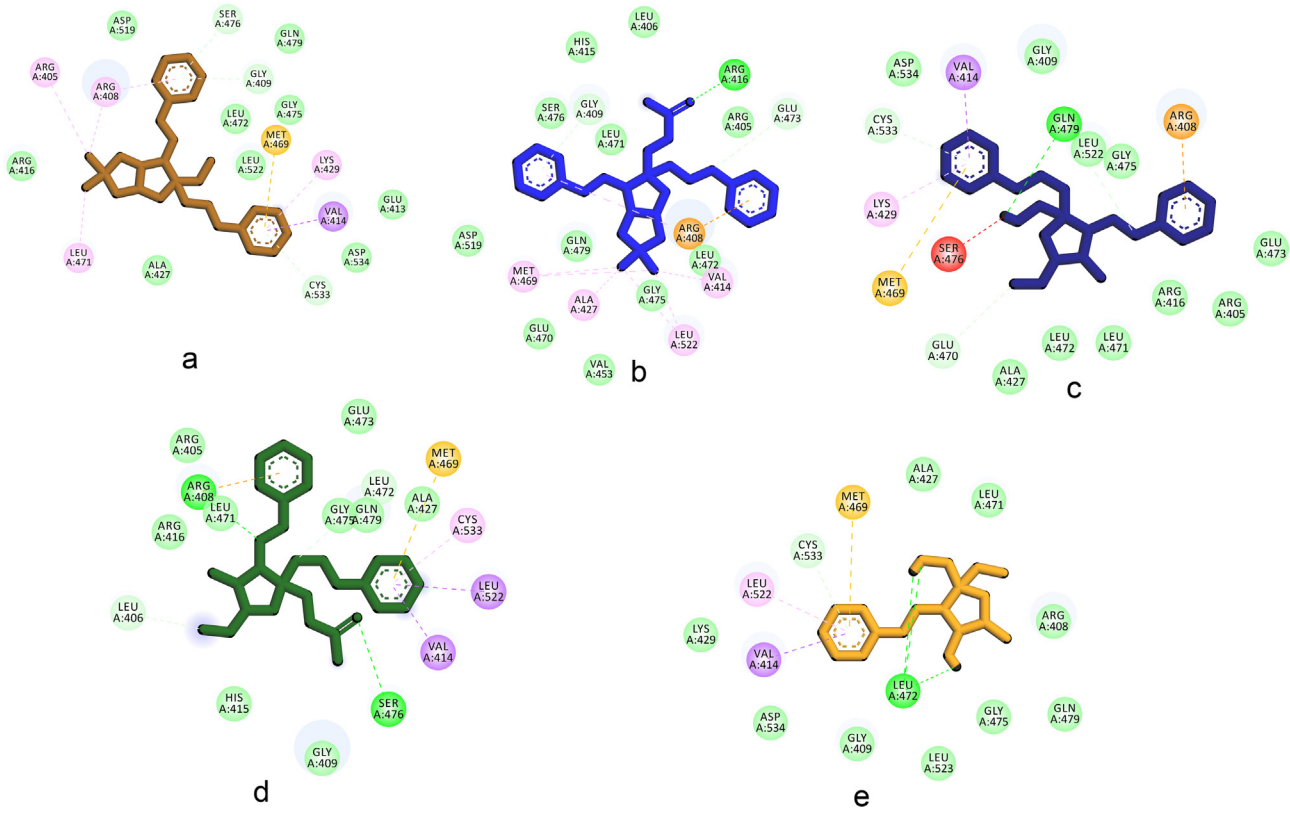

Fig. 6. Interaction of synthesized compounds (a) **2**, (b) **3**, (c) **4**, (d) **5** and (e) **6** with NIK (4IDV) active site. Green: conventional hydrogen bond; pink-violet: hydrophobic; light green: Van der Waals; cyan: carbon hydrogen bond/ pi-donor hydrogen bond; orange: pi-cation; brown: pi-sulfur; red: electron donor–donor interaction.

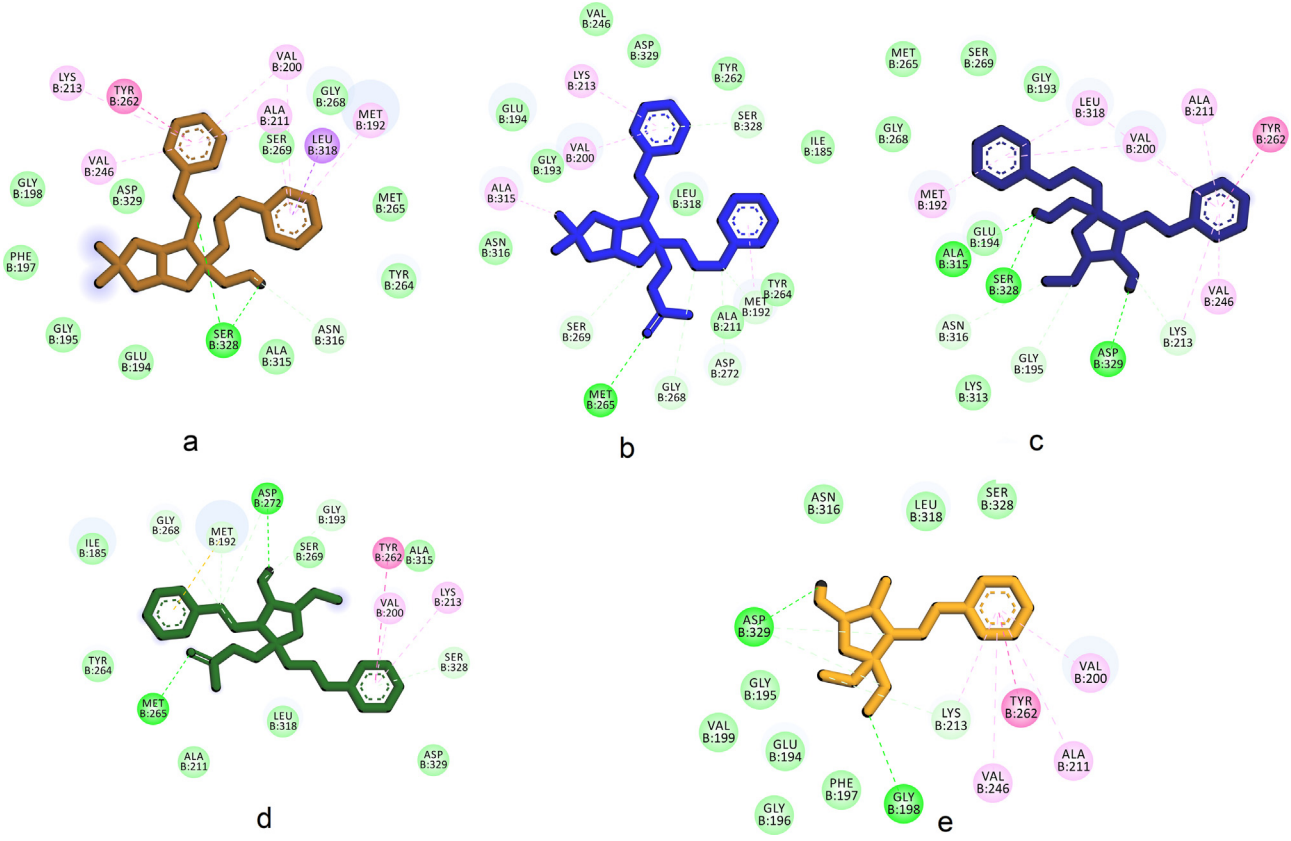

Fig. 7. Interaction of synthesized compounds (a) **2**, (b) **3**, (c) **4**, (d) **5** and (e) **6** with IRAK-4 (5KX7) active site. Green: conventional hydrogen bond; pink-violet: hydrophobic; light green: Van der Waals; cyan: carbon hydrogen bond/ pi-donor hydrogen bond interaction.

Table 3
Binding affinities of native ligands and synthesized compounds against target proteins.

Protein (PDB code)	Binding Affinity (kcal/mol)					
	Native ligand*	**2**	**3**	**4**	**5**	**6**
PLA_2 (4UY1)	−7.6	−8.5	−8.9	−8.6	−8.1	−7.2
COX-1 (1EQG)	−7.7	−6.2	−8.1	−7.4	−7.0	−7.0
COX-2 (5IKT)	−8.6	−5.4	−6.4	−6.5	−6.0	−6.1
NIK (4IDV)	−9.9	−8.2	−7.8	−7.3	−8.0	−7.0
IRAK-4 (5KX7)	−8.7	−9.1	−8.9	−8.3	−8.2	−6.9

* Native ligands of PLA_2 (4UY1), COX-1 (1EQG), COX-2 (5IKT), NIK (4IDV), IRAK-4 (5KX7) are 5-(2,5-dimethyl-3-thienyl)-1h-pyrazole-3-carboxamide (PubChem CID: 78673871), ibuprofen (PubChem CID: 3672), tolfenamic acid (PubChem CID: 610479), 4-{3-[2-amino-5-(2-methoxyethoxy)pyrimidin-4-yl]-1h-indol-5-yl}-2-methylbut-3-yn-2-ol (PubChem CID: 58221375), {n}-(3-aminocarbonyl-1-methyl-pyrazol-4-yl)-6-(1-methylpyrazol-4-yl)pyridine-2-carboxamide (PubChem CID: 316933309), respectively.

Table 4
Drug-like property prediction of the synthesized compounds (Lipinski's rule of five).

Compounds (ligands)	Molecular weight	Acceptor of H-bond	Donor of H-bond	Molar Refractivity	LogP	No. of Violations
2	400.46	6	1	106.40	1.16	0
3	442.50	7	0	116.14	1.91	0
4	373.43	6	2	98.94	0.72	0
5	416.46	7	1	108.68	1.09	0
6	270.28	6	4	64.99	−0.95	0

Acceptance criteria: molecular weight < 500, octanol–water partition coefficient (expressed as LogP) < 5, number of hydrogen bond donor $\leq$ 5, number of hydrogen bond acceptor $\leq$ 10, molar refractivity between 40 and 130.

of the synthesized compounds with ribose and its nucleosides with analgesic effect favors the results of anti-nociceptive tests. However, to understand the mechanism by which these compounds exhibit analgesic effects need more study and further structural modifications of these compounds may lead to better analgesics.

Carrageenan induced paw edema test was carried out on laboratory animals to observe the anti-inflammatory effect of the compounds. Intra plantar injection of 1% carrageenan induces local edema that increases with time releasing different inflammatory mediators in two phases. In the first phase that may last up to 1.5 h after injection of carrageenan involves the release of histamine, 5-hydroxytryptamine, platelet activating factor, bradykinin whereas in the second phase prostaglandin and various cytokines dominates (Mehrzadi et al., 2020). All the compounds exhibited promising anti-inflammatory activity with paw edema inhibition ranging from 78.32% to 95.15% in 4th hour. Anti-inflammatory effects of compound **3**, **4**, **5** and **6** are reported for the first time in the current study. Since the synthesized compounds exhibited considerable anti-inflammatory effect, we may assume that the compounds may interact with the inflammatory mediators or interfere in any of the mechanistic pathways associated with these mediators such as antagonistic action on these mediator's receptor or interference in the biosynthesis procedure of these mediators. The observed activity of the compounds might be rationalized that the compounds are derivatives of D-ribose and possess structural similarity to some adenosine kinase inhibitors both of which displayed anti-inflammatory activity (Jarvis et al., 2002; Ueki et al., 2013). Therefore, the compounds might represent as credible leads for the development of potential anti-inflammatory agents via further structural modifications and screening.

Biological evaluation of our synthesized compounds showed considerable analgesic and anti-inflammatory activity. In order to reinforce the results of the biological studies and to get some idea about the biological targets of the synthesized compounds, docking against some proteins important for pain and inflammation were accomplished. Molecular docking of our synthesized compounds was done against phospholipase A_2 (PLA_2), cyclooxygenase-1 (COX-1), cyclooxygenase-2 (COX-2), NF-κB–inducing kinase (NIK) and interleukin-1 receptor-associated kinase-4 (IRAK-4) all of which have a significant role in inflammation and pain. Both COX-1 and COX-2, act as a catalyst the formation of prostaglandins, prostacyclines, thromboxanes and are targets of non-steroidal anti-inflammatory agents (Chandrasekharan and Simmons, 2004). PLA_2 enzymes have roles in the arachidonic acid metabolic pathway and biosynthesis of eicosanoid in both physiological condition and in inflammation (Burke and Dennis, 2009). NIK is commonly related to signaling mechanism of various cytokines and regulation of inflammation-angiogenesis (Pflug and Sitcheran, 2020). IRAK-4, a protein kinase, is necessary in numerous inflammatory signaling pathways (Lye et al., 2004). Synthesized compounds showed efficient binding with these molecular targets. Compound **2** had higher binding affinities toward COX-1 and NIK than the corresponding native ligands. Compound **3** interacted with Arg120A residue of COX-1 which is required for high affinity binding of arachidonic acid with cyclooxygenase (Vecchio et al., 2012). Compound **3** also interacted with PLA_2 and IRAK-4 active site effectively and these interactions may be accounted for significant anti-inflammatory and analgesic activity of this compound in biological study.

Lipinski's rule of five illustrates molecular properties of candidate compounds related to pharmacokinetics for successful outcomes in drug development process. It indicates that when a molecule transgresses these rules it is likely to have poor pharmacokinetic property and not favorable as a lead for drug development (Lipinski, 2004). All synthesized compounds complied with acceptable criteria, therefore, these compounds may have good pharmacokinetic properties for consideration in drug development (Wang et al., 2015).

5. Conclusion

In conclusion, five α-D-ribofuranose analogues were synthesized and evaluated for their pharmacological potential. The compound **3** manifested significant analgesic effect in peripheral and central analgesic assay whereas the other analogues demonstrated mild to moderate analgesic activity. In carrageenan-induced hind paw edema method both **2** and **6** exerted significant anti-inflammatory effect. In molecular docking study, compound **3**

showed highest binding affinity with COX-1, COX-2 and PLA_2 whereas compound **2** manifested highest binding affinity with NIK and IRAK-4. Further study and structural modifications are required to learn more about the biological properties and underlying mechanisms which is the subject of our future investigation.

Funding

This work was supported by the Ministry of Science, Information and Communication Technology, Government of the People's Republic of Bangladesh (grant no. 39.00.0000.012.002.04.19.09).

Declaration of Competing Interest

The authors declare that they have no known competing financial interests or personal relationships that could have appeared to influence the work reported in this paper.

References

Adamo, M., Pergoli, R., 2008. Synthesis and medicinal properties of 2-deoxyribose and ribose C-nucleoside. Curr. Org. Chem. 12, 1544–1569. https://doi.org/10.2174/138527208786786318.

Adukwu, E.C., Bowles, M., Edwards-Jones, V., Bone, H., 2016. Antimicrobial activity, cytotoxicity and chemical analysis of lemongrass essential oil (Cymbopogon flexuosus) and pure citral. Appl. Microbiol. Biotechnol. 100 (22), 9619–9627. https://doi.org/10.1007/s00253-016-7807-y.

Ahmed, S., Al-Rehaily, A.J., Alam, P., Alqahtani, A.S., Hidayatullah, S., Rehman, M.T., Mothana, R.A., Abbas, S.S., Khan, M.U., Khalid, J.M., Siddiqui, N.A., 2019. Antidiabetic, antioxidant, molecular docking and HPTLC analysis of miquelianin isolated from Euphorbia schimperi C. Presl. Saudi Pharm. J. 27 (5), 655–663. https://doi.org/10.1016/j.jsps.2019.03.008.

Berman, H.M., Battistuz, T., Bhat, T.N., Bluhm, W.F., Bourne, P.E., Burkhardt, K., Feng, Z., Gilliland, G.L., Iype, L., Jain, S., Fagan, P., Marvin, J., Padilla, D., Ravichandran, V., Schneider, B., Thanki, N., Weissig, H., Westbrook, J.D., Zardecki, C., 2002. The protein data bank. Acta Crystallogr. Sect. D Biol. Crystallogr. 58 (6), 899–907. https://doi.org/10.1107/S0907444902003451.

Burke, J.E., Dennis, E.A., 2009. Phospholipase A 2 structure/function, mechanism, and signaling. ASBMB. 50, S237–S242. https://doi.org/10.1194/jlr.R800033-JLR200.

Cappellacci, L., Barboni, G., Palmieri, M., Pasqualini, M., Grifantini, M., Costa, B., Martini, C., Franchetti, P., 2002. Ribose-modified nucleosides as ligands for adenosine receptors: synthesis, conformational analysis, and biological evaluation of 1′-C-Methyl adenosine analogues. J. Med. Chem. 45, 1196–1202. https://doi.org/10.1021/jm0102755.

Chandrasekharan, N.V., Simmons, D.L., 2004. The cyclooxygenases. Genome Biol. 5, 1–7. https://doi.org/10.1186/gb-2004-5-9-241.

Chung, S.-T., Huang, W.-H., Huang, C.-K., Liu, F.-C., Huang, R.-Y., Wu, C.-C., Lee, A.-R., 2016. Synthesis and anti-inflammatory activities of 4H-chromene and chromeno[2,3-b]pyridine derivatives. Res. Chem. Intermed. 42 (2), 1195–1215. https://doi.org/10.1007/s11164-015-2081-7.

Daina, A., Michielin, O., Zoete, V., 2017. SwissADME: A free web tool to evaluate pharmacokinetics, drug-likeness and medicinal chemistry friendliness of small molecules. Sci. Rep. 7, 1–13. https://doi.org/10.1038/srep42717.

Downey, A.M., Richter, C., Pohl, R., Mahrwald, R., Hocek, M., 2015. Direct one-pot synthesis of nucleosides from unprotected or 5-O-monoprotected D -ribose. Org. Lett. 17, 4604–4607. https://doi.org/10.1021/acs.orglett.5b02332.

Dzoyem, J.P., McGaw, L.J., Kuete, V., Bakowsky, U., 2017. Anti-inflammatory and anti-nociceptive activities of African medicinal spices and vegetables. In: Medicinal spices and vegetables from Africa: Therapeutic potential against metabolic, inflammatory, infectious and systemic Diseases. Elsevier Inc., pp. 239–270. https://doi.org/10.1016/B978-0-12-809286-6.00009-1.

El-Gazzar, A.-R., Hafez, H.N., Abbas, H.-A., 2009. S- and C-nucleosidoquinazoline as new nucleoside analogs with potential analgesic and anti-inflammatory activity. Eur. J. Med. Chem. 44 (10), 4249–4258. https://doi.org/10.1016/j.ejmech.2009.05.025.

Faujdar, S., Sharma, S., Sati, B., Pathak, A.K., Paliwal, S.K., 2016. Comparative analysis of analgesic and anti-inflammatory activity of bark and leaves of Acacia ferruginea DC. Beni-Suef Univ. J. Basic Appl. Sci. 5 (1), 70–78. https://doi.org/10.1016/j.bjbas.2016.02.002.

Ferreira, S., Sodero, A.C.R., Cardoso, M.F.C., Lima, E.S., Kaiser, C.R., Silva, F.P., Ferreira, V.F., 2010. Synthesis, biological activity and molecular modeling studies of 1H–1,2,3-triazole derivatives of carbohydrates as α-glucosidases nhibitors. J. Med. Chem. 53, 2364–2375. https://doi.org/10.1021/jm901265h.

Fujisaka, A., Hari, Y., Takuma, H., Rahman, S.M.A., Yoshikawa, H., Pang, J., Imanishi, T., Obika, S., 2019. Effective syntheses of 2′, 4′-BNANC monomers bearing adenine, guanine, thymine, and 5-methylcytosine, and the properties of oligonucleotides fully modified with 2′, 4′-BNANC. Bioorg. Med. Chem. 27 (8), 1728–1741. https://doi.org/10.1016/j.bmc.2019.02.034.

Galmarini, C., Popowycz, F., Joseph, B., 2008. Cytotoxic nucleoside analogues: different strategies to improve their clinical efficacy. Curr. Med. Chem. 15, 1072–1082. https://doi.org/10.2174/092986708784221449.

Gebhart, B., Jorgenson, J.A., 2004. Benefit of ribose in a patient with fibromyalgia. Pharmacotherapy. 24 (11), 1646–1648. https://doi.org/10.1592/phco.24.16.1646.50957.

Hari, Y., Obika, S., Sakaki, M., Morio, K.-I., Yamagata, Y., Imanishi, T., 2002. Effective synthesis of C-nucleosides with 2′,4′-BNA modification. Tetrahedron. 58 (15), 3051–3063. https://doi.org/10.1016/S0040-4020(02)00226-0.

Jarvis, M.F., Yu, H., McGaraughty, S., Wismer, C.T., Mikusa, J., Zhu, C., Chu, K., Kohlhaas, K., Cowart, M., Lee, C.H., Stewart, A.O., Cox, B.F., Polakowski, J., Kowaluk, E.A., 2002. Analgesic and anti-inflammatory effects of A-286501, a novel orally active adenosine kinase inhibitor. Pain. 96, 107–118. https://doi.org/10.1016/S0304-3959(01)00435-3.

Komatsu, H., Araki, T., 2003. Chemo-enzymatic synthesis of 2′,3′-dideoxy-3′-fluoro-β-D-guanosine via 2,3-dideoxy-3-fluoro-α-D-ribose 1-phosphate. Tetrahedron Lett. 44 (14), 2899–2901. https://doi.org/10.1016/S0040-4039(03)00428-3.

Koshkin, A.A., Singh, S.K., Nielsen, P., Rajwanshi, V.K., Kumar, R., Meldgaard, M., Olsen, C.E., Wengel, J., 1998. LNA (Locked Nucleic Acids): synthesis of the adenine, cytosine, guanine, 5-methylcytosine, thymine and uracil bicyclonucleoside monomers, oligomerisation, and unprecedented nucleic acid recognition. Tetrahedron. 54 (14), 3607–3630. https://doi.org/10.1016/S0040-4020(98)00094-5.

Kumar, N., Singh, G., Yadav, A.K., 2001. Synthesis of some new pyrido[2,3-d] pyrimidines and their ribofuranosides as possible antimicrobial agents. Heteroat. Chem. 12, 52–56. https://doi.org/10.1002/1098-1071(2001)12:1<52::AID-HC11>3.0.CO;2-0.

Leksiri, S., Hasriadi, H., Dasuni Wasana, P.W., Vajragupta, O., Rojsitthisak, P., Towiwat, P., 2020. Co-administration of pregabalin and curcumin synergistically decreases pain-like behaviors in acute nociceptive pain murine models. Molecules. 25, 4172. https://doi.org/10.3390/molecules25184172.

Lipinski, C.A., 2004. Lead- and drug-like compounds: The rule-of-five revolution. Drug Discov. Today Technol. 1 (4), 337–341. https://doi.org/10.1016/j.ddtec.2004.11.007.

Lye, E., Mirtsos, C., Suzuki, N., Suzuki, S., Yeh, W.-C., 2004. The role of interleukin 1 receptor-associated kinase-4 (IRAK-4) kinase activity in IRAK-4-mediated signaling. ASBMB. 279 (39), 40653–40658. https://doi.org/10.1074/jbc.M402666200.

Mehrzadi, S., Khalili, H., Fatemi, I., Malayeri, A., Siahpoosh, A., Goudarzi, M., 2020. Zingerone mitigates carrageenan-induced inflammation through antioxidant and anti-inflammatory activities. Inflammation 44, 186–193. https://doi.org/10.1007/s10753-020-01320-y.

O'Boyle, N.M., Banck, M., James, C.A., Morley, C., Vandermeersch, T., Hutchison, G.R., 2011. Open Babel: an open chemical toolbox. J. Cheminform. 3, 33. https://doi.org/10.1186/1758-2946-3-33.

Omran, H., Illien, S., MacCarter, D., St. Cyr, J., Lüderitz, B., 2003. D-Ribose improves diastolic function and quality of life in congestive heart failure patients: a prospective feasibility study. Eur. J. Heart Fail. 5, 615–619. https://doi.org/10.1016/S1388-9842(03)00060-6.

Petrelli, R., Scortichini, M., Kachler, S., Boccella, S., Cerchia, C., Torquati, I., Del Bello, F., Salvemini, D., Novellino, E., Luongo, L., Maione, S., Jacobson, K.A., Lavecchia, A., Klotz, K.N., Cappellacci, L., 2017. Exploring the role of N6-substituents in potent dual acting 5′-C-ethyltetrazolyladenosine derivatives: synthesis, binding, functional assays, and antinociceptive effects in mice. J. Med. Chem. 60, 4327–4341. https://doi.org/10.1021/acs.jmedchem.7b00291.

Pflug, K.M., Sitcheran, R., 2020. Targeting NF-κB-inducing kinase (NIK) in immunity, inflammation, and cancer. Int. J. Mol. Sci. 21, 8470. https://doi.org/10.3390/ijms21228470.

Rahman, F.I., Hussain, F., Saqueeb, N., Rahman, S.M.A., 2020. Synthesis and evaluation of pharmacological activities of some 3-O-benzyl-4-C-(hydroxymethyl)-1,2-O-isopropylidene-α-D-ribofuranose derivatives as potential anti-inflammatory agents and analgesics. Res. Pharm. Sci. 15, 209–217. https://doi.org/10.4103/1735-5362.288423.

Rahman, S.M.A., Imanishi, T., Obika, S., 2009. Synthesis of several types of bridged nucleic acids. Chem. Lett. 38 (6), 512–517. https://doi.org/10.1246/cl.2009.512.

Rahman, S.M.A., Seki, S., Obika, S., Yoshikawa, H., Miyashita, K., Imanishi, T., 2008. Design, synthesis, and properties of 2′,4′-BNANC: a bridged nucleic acid analogue. J. Am. Chem. Soc. 130, 4886–4896. https://doi.org/10.1021/ja710342q.

Sharma, V.K., Rungta, P., Maikhuri, V.K., Prasad, A.K., 2015. An astute synthesis of locked nucleic acid monomers. Sustain. Chem. Process. 3, 1–6. https://doi.org/10.1186/s40508-015-0028-3.

Shecterle, L.M., Terry, K.R., Cyr St., J.A., 2010. The patented uses of D-ribose in cardiovascular diseases. Recent Pat. Cardiovasc. Drug Discov. 5, 138–142. https://doi.org/10.2174/157489010791515241.

Teitelbaum, J., 2012. Treatment of chronic fatigue syndrome and fibromyalgia with D-ribose-an open-label, multicenter study. Open Pain J. 5 (1), 32–37. https://doi.org/10.2174/1876386301205010032.

Trott, O., Olson, A.J., 2009. AutoDock Vina: Improving the speed and accuracy of docking with a new scoring function, efficient optimization, and multithreading. J. Comput. Chem. 31, 455–461. https://doi.org/10.1002/jcc.21334.

Ueki, Masaaki, Ueno, Masaki, Morishita, Jun, Maekawa, Nobuhiro, 2013. D-ribose ameliorates cisplatin-induced nephrotoxicity by inhibiting renal inflammation

in mice. Tohoku J. Exp. Med. 229 (3), 195–201. https://doi.org/10.1620/tjem.229.195.
Vecchio, Alex J., Orlando, Benjamin J., Nandagiri, Ritwik, Malkowski, Michael G., 2012. Investigating substrate promiscuity in cyclooxygenase-2 the role of Arg-120 and residues lining the hydrophobic groove. J. Biol. Chem. 287 (29), 24619–24630. https://doi.org/10.1074/jbc.M112.372243.
Wagner, S., Herrick, J., Shecterle, L.M., St. Cyr, J.A., 2009. D-ribose, a metabolic substrate for congestive heart failure. Prog. Cardiovasc. Nurs. 24, 59–60. https://doi.org/10.1111/j.1751-7117.2009.00033.x.
Wang, Y., Xing, J., Xu, Y., Zhou, N., Peng, J., Xiong, Z., Liu, X., Luo, X., Luo, C., Chen, K., Zheng, M., Jiang, H., 2015. In silico ADME/T modelling for rational drug design. Q. Rev. Biophys. 48, 488–515. https://doi.org/10.1017/S0033583515000190.
Zhang, Bin, Wu, Jia-Ting, Zheng, Cai-Juan, Zhou, Xue-Ming, Yu, Zhang-Xin, Li, Wan-Shan, Chen, Guang-Ying, Zhu, Guo-Yuan, 2021. Bioactive cyclohexene derivatives from a mangrove-derived fungus Cladosporium sp. JJM22. Fitoterapia. 149, 104823. https://doi.org/10.1016/j.fitote.2020.104823.